


Synthesis, computational study, solvatochromism and biological studies of thiazole-owing hydrazone derivatives

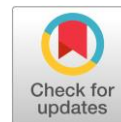
C. Kiran Yadav ^a, B.P. Nandeshwarappa ^{a*} , K.M. Mussuvir Pasha ^b

a: Department of Studies in Chemistry, Shivagangotri, Davangere University, Davanagere, Karnataka 577007, India

b: Department of P.G. studies and research in chemistry/Industrial chemistry, Vijayanagara Sri Krishnadevaraya University, Ballari 583105, Karnataka, India

* Corresponding author: belakatte@gmail.com

This paper belongs to a Regular Issue.



Abstract

In the present work, we have synthesized thiazole-hydrazone conjugates **5(a-h)** and characterized them using various analytical techniques such as UV, IR, NMR, and mass spectrometry. Solvatochromic properties were evaluated in ten solvents with different polarity and quantum chemical parameters using a DFT study. The antibacterial activity results revealed that compounds **5c**, **5d** and **5g** exhibited good efficacy and that the remaining compounds displayed significant activity. The synthesized compounds were screened for their cytotoxic activity against HepG2 and MCF-7 cell lines, and all the synthesized compounds exhibited significant potency towards the screened cancer cell lines. The anti-inflammatory efficacy of the synthesized thiazole derivatives was determined against MMP-2 and MMP-9, and some of the compounds showed significant activity. Furthermore, the *in silico* molecular docking was performed with the COX-2 receptor.

Key findings

- Thiazole-hydrazone conjugates were synthesized. Biological efficacy of the synthesized compounds was determined.
- Solvatochromic properties were evaluated in ten different solvents. Structures were characterized by using various analytical techniques.
- Quantum chemical parameters were evaluated using a DFT study.

© 2023, the Authors. This article is published in open access under the terms and conditions of the Creative Commons Attribution (CC BY) license (<http://creativecommons.org/licenses/by/4.0/>).

Keywords

biological activity
DFT
solvatochromic study
thiazole-hydrazone
conjugates

Received: 18.01.23

Revised: 05.02.23

Accepted: 10.02.23

Available online: 20.02.23



1. Introduction

Heterocyclic compounds are important for medicinal chemistry because they serve as key building blocks for active pharmaceutical ingredients. Compounds with heterocyclic ring systems are extremely useful in both medicine and material science [1–5]. Thiazoles, for example, are five-membered ring heterocycles with three carbon atoms, one nitrogen atom, and one sulfur atom. These heterocycles are of great interest in medicinal and pesticide chemistry, as well as polymer and material science [6]. Thiazoles are one of the most important classes of heterocyclic moieties which possess a wide range of therapeutic and pharmacological applications. Compounds containing thiazole ring have chemotherapeutic, fungicidal, and pesticidal properties [7–11]. Thiazole derivatives have broad biological activities such as antimicrobial [12], anti-inflammatory [13],

antitubercular [14], antihypertensive [15], anticancer [16], and analgesic [17]. Natural compounds such as thiamine, thiamine pyrophosphate, bacitracin, penicillin antibiotics, and most of the drugs contain thiazole moiety. From the recent literature survey, thiazole and its derivatives were used as antimicrobial additives in polyurethane coating, and their corrosion behavior was also investigated [18, 19]. An asymmetric thiazole core exhibits fascinating behavior such as nonlinear optical properties and ferroelectricity with a lateral π -conjugated system [20]. Thiazole-based fluorophores are used as blue light-emitting polymers in organic light-emitting diodes (OLEDs); thiazoles are also used in dye synthesized solar cells [21]. Hydrazones and their derivatives are organic compounds with a wide range of applications. The biological properties of these compounds are intriguing. Hydrazones are useful as potential ligands for metal complexes, organocatalysis, and the synthesis of heterocyclic

compounds [22–25]. The complex study of hydrazones has piqued interest due to their biological activity and potential as enzyme inhibitors. Hydrazones' rings are crucial in determining the magnitude of their pharmacological properties [26, 27]. Hydrazones can act as neutral or anionic ligands for metal ions, resulting in stable metal complexes. These hydrazones have revealed themselves to be important optical phenomena materials [28].

2. Experimental details

2.1. Materials and methods

All the chemicals and solvents were purchased from Sigma-Aldrich and Spectrochem. The FT-IR spectra were recorded on a Perkin Elmer spectrometer (Spectrum 100). The electronic absorption spectra were recorded on a Shimadzu spectrophotometer (UV-1800). The ^1H NMR and ^{13}C NMR spectra were recorded with the aid of an Agilent NMR at 400 MHz and 100 MHz, respectively. The HR-MS spectra were recorded on a Sciex API 3200 mass spectrometer. Melting points were determined in open capillary and are uncorrected. Silica-gel GF-254 was used for thin-layer chromatography (TLC). Purity of the compounds was checked by TLC on silica gel. All extracted solvents were dried with anhydrous Na_2SO_4 and evaporated with a BUCHI rotary evaporator.

2.2. Computational studies

All computational calculations were performed using the Gaussian 09 software [29], and B3LYP was used for the DFT calculations with a 6-31G (d, p) basis set [30, 31]. Output files of the Gaussian software were visualized by using Gaussview 05 [32]. MEP and RDG calculations were done using Multiwfn 3.7 [32] and visualized using Visual Molecular Dynamics (VMD) software [33].

2.3. General procedure for the synthesis of thiazole hydrazones 5(a–h)

2.3.1. Step 1: synthesis of thiosemicarbazones 3(a–h)

2 mmol of various carbonyl compounds **1(a–h)** and 2 mmol of thiosemicarbazide **2** were taken in 10 mL of ethanol and stirred with reflux at 70–80 °C in oil bath for about 1–2 hrs, employing 2–3 drops of AcOH catalyst. After the complete formation of the product identified by TLC (Mobile phase: n-Hexane:Ethyl acetate 8:2), the obtained solid was filtered, washed with ethanol, dried and recrystallised using ethanol solvent.

2.3.2. Step 2: synthesis of thiazole hydrazones 5(a–h)

1 mmol of the obtained thiosemicarbazones **3(a–h)** from step 1, and phenacyl bromide (1 mmol) were taken together in 50 mL RB; to that, 10–15 mL of isopropanol was added, and the mixture was stirred at room temperature for about 2–3 hrs. The formation of the product was monitored by TLC (Mobile phase: n-Hexane:Ethyl acetate 8:2). After the

completion of the reaction, the obtained colorant was filtered, dried, and recrystallized using ethanol.

2.3.3. 2-((2E)-2-[4-fluoro-3-(trifluoromethyl)benzylidene]hydrazinyl)-4-phenyl-1,3-thiazole (5a)

$\text{C}_{17}\text{H}_{11}\text{F}_4\text{N}_3\text{S}$, m.p: 187–189 °C. FT-IR (KBr) ν_{max} : 3066 (N–H), 1582 (C=N), 1484 (C=N), 1278 (C–F), 709 (C–S). ^1H NMR (400 MHz, $\text{DMSO}-d_6$) δ in ppm 7.31 (t, 1H, ArH, $J = 7.6$ Hz), 7.36 (s, 1H, ArH), 7.41 (d, 2H, ArH, $J = 8$ Hz), 7.58 (t, 1H, ArH, $J = 8$ Hz), 7.85 (d, 2H, ArH, $J = 8$ Hz), 8.04 (t, 2H, ArH, $J = 8$ Hz), 8.11 (s, 1H, ArH), 12.40 (s, 1H, N–NH). ^{13}C NMR (100 MHz, $\text{DMSO}-d_6$): δ 103.97, 117.81, 121.10, 123.80, 124.65, 125.51, 127.56, 128.59, 131.77, 132.29, 134.57, 138.43, 150.61, 157.60, 160.14, 168.01. HRMS: $m/z = 365.8$ [M^+]. Anal. Calcd (%): C (55.89%), H (3.03%), N (11.50%), Found: C (55.35), H (2.98), N (11.12).

2.3.4. 2-[(2E)-2-(2,6-dibromobenzylidene)hydrazinyl]-4-phenyl-1,3-thiazole (5b)

$\text{C}_{16}\text{H}_{11}\text{Br}_2\text{N}_3\text{S}$, m.p: 192–193 °C. FT-IR (KBr) ν_{max} : 3317 (N–H), 1633 (C=N), 1546 (C=N), 725 (C–S), 608 (C–Br). ^1H NMR (400MHz, $\text{DMSO}-d_6$) δ in ppm 7.23 (t, 1H, ArH, $J = 8$ Hz), 7.33 (t, 2H, ArH, $J = 7.2$ Hz), 7.41 (t, 2H, ArH, $J = 8$ Hz), 7.81 (d, 2H, ArH, $J = 8$ Hz), 7.86 (t, 2H, ArH, $J = 7.6$ Hz), 8.15 (s, 1H, ArH), 12.30 (s, 1H, N–NH). ^{13}C NMR (100 MHz, $\text{DMSO}-d_6$): δ 104.31, 123.20, 125.65, 127.76, 127.91, 128.37, 128.62, 131.33, 132.74, 133.09, 134.16, 139.70, 149.83, 168.16. HRMS: $m/z = 436.0$ [$\text{M}-1$]. Anal. Calcd (%): C (43.96%), H (2.54%), N (9.61%), Found: C (43.45), H (2.24), N (9.27).

2.3.5. 4-((E)-[2-(4-phenyl-1,3-thiazol-2-yl)hydrazinylidene]methyl}benzaldehyde (5c)

$\text{C}_{17}\text{H}_{13}\text{N}_3\text{OS}$, m.p: 171–173 °C. FT-IR (KBr) ν_{max} : 3299 (N–H), 1689 (C=N), 1569 (C=N), 712 (C–S). ^1H NMR (400MHz, $\text{DMSO}-d_6$) δ in ppm 7.1 (s, 1H, ArH), 7.26 (m, 2H ArH, $J = 7.2$ Hz), 7.38 (m, 2H, ArH, $J = 8$ Hz), 7.72 (s, 1H, ArH), 7.75 (m, 1H, ArH, $J = 8$ Hz), 7.83 (m, 3H, ArH, $J = 4$ Hz), 8.03 (s, 1H, ArH), 9.94 (s, 1H, –CHO). ^{13}C NMR (100 MHz, $\text{DMSO}-d_6$): δ 38.87, 40.12, 104.11, 125.68, 126.77, 128.03, 128.79, 130.20, 134.78, 135.22, 139.44, 140.83, 150.72, 168.42, 192.63. HRMS: $m/z = 308.1$ [$\text{M}+1$]. Anal. Calcd (%): C (66.43%), H (4.26%), N (13.67%), Found: C (66.12), H (4.06), N (13.16).

2.3.6. 2-((2E)-2-[4-(methylsulfanyl)benzylidene]hydrazinyl)-4-phenyl-1,3-thiazole (5d)

$\text{C}_{17}\text{H}_{15}\text{N}_3\text{S}_2$, m.p: 189–191 °C. FT-IR (KBr) ν_{max} : 3054 (N–H), 1595 (C=N), 1494 (C=N), 712 (C–S). ^1H NMR (400MHz, $\text{DMSO}-d_6$) δ in ppm: 2.50 (t, 3H, – CH_3), 7.30 (t, 4H, ArH, $J = 1.2$ Hz), 7.41 (t, 2H, ArH, $J = 8$ Hz), 7.60 (d, 2H, ArH, $J = 4.4$ Hz), 7.86 (d, 2H, ArH, $J = 7.2$ Hz), 7.99 (s, 1H, ArH), 12.01 (s, 1H, N–NH). ^{13}C NMR (100 MHz, $\text{DMSO}-d_6$): δ 14.35, 40.12, 103.54, 125.48, 126.64, 127.46, 128.56, 130.90, 134.62, 139.82, 140.89, 150.43, 168.16. HRMS: $m/z =$ Anal. Calcd (%): C (62.74%), H (4.65%), N (12.91%), Found: C (62.41), H (4.35), N (12.62).

2.3.7. 2-{2-[1-(furan-2-yl)ethylidene]hydrazinyl}-4-phenyl-1,3-thiazole (5e)

$C_{15}H_{13}N_3OS$, m.p: 135–136 °C. FT-IR (KBr) ν_{max} : 3088 (N-H), 1612 (C=N), 1496 (C=N), 719(C-S). 1H NMR (400 MHz, DMSO- d_6) δ in ppm 2.25 (s, 3H, $-CH_3$), 6.58 (m, 2H, ArH, $J = 1.6$ Hz), 6.84 (d, 1H, ArH, $J = 3.2$ Hz), 7.31 (d, 2H, ArH, $J = 5.6$ Hz), 7.41 (t, 2H, ArH, $J = 8$ Hz), 7.77 (d, 1H, ArH, $J = 1.2$ Hz), 7.88 (t, 2H, ArH, $J = 7.2$ Hz), 11.30 (s, 1H, N-NH). ^{13}C NMR (100 MHz, DMSO- d_6): δ 13.85, 40.12, 104.17, 110.17, 111.89, 125.59, 127.68, 128.06, 128.64, 134.18, 139.66, 144.13, 151.66, 169.41. HRMS: $m/z = 283.80$ [M^+]. Anal. Calcd (%): C (63.58%), H (4.62%), N (14.83%), Found: C (63.37), H (4.28), N (14.57).

2.3.8. 4-phenyl-2-[(2E)-2-(1-phenylpropylidene)hydrazinyl]-1,3-thiazole (5f)

$C_{18}H_{17}N_3S$, m.p: 159–160 °C. FT-IR (KBr) ν_{max} : 3062 (N-H), 1617 (C=N), 1494 (C=N), 769 (C-S). 1H NMR (400 MHz, DMSO- d_6) δ in ppm 1.09 (t, 3H, $-CH_3$), 2.88 (m, 2H, $-CH_2$), 7.32 (d, 2H, ArH, $J = 7.2$ Hz), 7.42 (m, 5H, ArH, $J = 7.6$ Hz), 7.80 (d, 2H, ArH, $J = 7.2$ Hz), 7.89 (d, 2H, ArH, $J = 7.2$ Hz), 11.30 (s, 1H, N-NH). ^{13}C NMR (100 MHz, DMSO- d_6): δ 8.08, 19.74, 31.20, 104.15, 125.59, 127.48, 128.11, 128.53, 128.65, 128.73, 129.03, 130.54, 132.96, 133.62, 136.35, 136.59, 168.63, 169.83. HRMS: $m/z = 309.10$ [$M+2$]. Anal. Calcd (%): C (70.33%), H (5.57%), N (13.67%), Found: C (70.10), H (5.38), N (13.52).

2.3.9. 2-[(2E)-2-[1-(4-ethylphenyl)ethylidene]hydrazinyl]-4-phenyl-1,3-thiazole (5g)

$C_{19}H_{19}N_3S$, m.p: 201–203 °C. FT-IR (KBr) ν_{max} : 3061 (N-H), 1614 (C=N), 1508 (C=N), 717 (C-S). 1H NMR (400 MHz, DMSO- d_6) δ in ppm 1.19 (m, 3H, $-CH_3$), 2.32 (s, 3H, $-CH_3$), 2.65 (m, 2H, $-CH_2$), 7.27 (t, 2H, ArH, $J = 8$ Hz), 7.32 (m, 2H, ArH, $J = 5.2$ Hz), 7.42 (t, 2H, ArH, $J = 8$ Hz), 7.70 (m, 2H, ArH, $J = 6$ Hz), 7.89 (d, 2H, ArH, $J = 7.2$ Hz), 11.10 (s, 1H, N-NH). ^{13}C NMR (100 MHz, DMSO- d_6): δ 14.61, 15.87, 39.30, 104.57, 126.27, 128.23, 128.77, 129.06, 134.44, 135.67, 145.16, 157.98, 170.28, 189.43, 215.73. HRMS: $m/z = 321.80$ [M^+]. Anal. Calcd (%): C (70.99%), H (5.96%), N (13.07%), Found: C (70.84), H (5.81), N (12.96).

2.3.10. 2-[(2E)-2-[1-(1,3-benzodioxol-5-yl)ethylidene]hydrazinyl]-4-phenyl-1,3-thiazole (5h)

$C_{18}H_{15}N_3O_2S$, m.p: 123–124 °C. FT-IR (KBr) ν_{max} : 3022 (N-H), 1599 (N-H), 1489 (N-H), 706 (C-S). 1H NMR (400 MHz, DMSO- d_6) δ in ppm 2.82 (s, 3H, $-CH_3$), 6.06 (s, 2H, $-CH_2$), 6.96 (d, 1H, ArH, $J = 8.4$ Hz), 7.27 (m, 1H, ArH, $J = 1.6$ Hz), 7.31 (d, 2H, ArH, $J = 7.6$ Hz), 7.35 (d, 2H, ArH, $J = 1.6$ Hz), 7.40 (m, 2H, ArH, $J = 8$ Hz), 7.88 (d, 2H, ArH, $J = 7.2$ Hz), 11.15 (s, 1H, N-NH). ^{13}C NMR (100 MHz, DMSO- d_6): δ 14.53, 39.30, 101.73, 104.33, 105.84, 108.35, 120.59, 125.94, 127.89, 129.01, 132.71, 135.16, 146.66, 148.37, 170.32, 223.72. HRMS:

$m/z = 338.10$ [$M+1$]. Anal. Calcd (%): C (64.08%), H (4.48%), N (12.45%), Found: C (59.97), H (4.36), N (12.32).

2.4. Biological activity

2.4.1. Antimicrobial activity

The antibacterial activity screening for synthesized compounds **5(a-h)** was done by the disc diffusion method [34–36]. The tubes were inoculated with 1ml lag phase culture of gram-negative bacteria such as *Escherichia coli*, *Pseudomonas aeruginosa*, and gram-positive bacteria such as *Staphylococcus aureus* and *Bacillus Subtilis*. Fungal strains such as *Candida albicans* and *Aspergillus flavus* were used. The sterile nutrient agar media was used for bacteria growth, and potato dextrose agar media was used for fungi. In the respective labeled discs, different concentrations (10–100 mg) of synthesized conjugates **5(a-h)** were added and mixed with DMSO. Then the bacterial plate was incubated at 37 °C for 24 hours and the fungal plate – at 27 °C for 48 hours. The zone of inhibition was measured for each compound.

2.4.2. Cytotoxic activity

Gibco Dulbecco's Modified Eagle Medium (DMEM) with 10% Fetal Bovine Serum was used to culture the cell line. The cytotoxic activity of the synthesized compounds was evaluated against MCF-7 and HePG2 cell lines using a modified micro-titration colorimetric MTT reduction method [37]. For 24 hours, cells were seeded at a density of $1 \cdot 10^4$ cells per well in 96-well plates. The cells were then exposed to various concentrations of synthesized compounds **5(a-h)** for 24 hours, ranging from 15.625 M to 1000 M. 10 μ L of MTT solution (5 mg/mL) was pipetted into each well and incubated for another 4h. The medium was discarded after the formazan precipitate was formed and dissolved in DMSO. The absorbance of the mixtures was measured at 570 nm with a microfilter plate reader, and cell viability was calculated.

$$\% \text{ inhibition} = [A_{\text{test}} / A_{\text{control}} \cdot 100], \quad (1)$$

where A_{test} is the absorbance of the test sample, A_{control} is the absorbance of control.

The IC_{50} value of the synthesized compounds was calculated using linear aggression equation, viz., $Y = Mx + C$. Here $Y = 50$ and M and C values were derived from the viability graph.

2.4.3. Anti-inflammatory activity

Gel electrophoresis was used to determine the anti-inflammatory efficacy of the prepared compounds against two matrix metalloproteinases, MMP-2 and MMP-9, as described in the published methodology [38]. Electrophoresis gels were prepared, and 50 liters of test compounds and 50 liters of MMP sample were thoroughly mixed before being incubated for one hour. Furthermore, the non-reducing buffer was thoroughly mixed in an equal-volume tank with the positive control (MMP) and negative control (tetracycline hydrochloride) (MMP). The tank was then closed and

plugged into a 50 V power supply for 15 minutes before increasing the voltage to 100 V until bromophenol blue reached the plate's bottom. The instrument was disconnected after completion, and the gel was gently removed, washed with a zymogram renaturing buffer solution for about 1 hour to remove SDS (sodium dodecyl sulfate), and allowed the proteins to denature. The zymogram renaturing buffer was decanted, and the gel was incubated overnight at 37 °C in the zymogram incubation buffer. Furthermore, the background stains blue with Coomassie stain where the Gelatin is degraded, and the gels are stained with Coomassie blue R-250. The presence of gelatinases is indicated by the development of white bands, with the lower bands being gelatinases-A (MMP-2) at 72 KD and the upper bands being gelatinases-B (MMP-9) at 95 KD.

2.4.4. *In silico* Molecular docking

The 2D structures of synthesized derivatives were drawn using ChemDraw. The energy was minimized using the Dundee prodrug server and then converted into PDBQT using the graphical interface program 'MGL tools' [39]. 3KCY is a crystal structure of Factor Inhibiting HIF-1 (FIH-1) with quinol family inhibitors at a resolution of 2.59 Å [40]. 'MGL tools' were used to adjust the grid box for docking simulations. The grid was adjusted so that it encompasses the region of the active site of the protein which comprised of Ile 281, Phe 207, His 279, Asp 201, Trp 296, His 199, Leu 186, Leu 188, Gln 147. The docking algorithm provided with AutodockVina was used to search for the best-docked conformation between ligand and protein, and the binding energy was determined. LigPlot and PyMol were used to infer the pictorial depiction of the interaction between the ligands and the target protein [41].

3. Results and Discussion

3.1. Chemistry and characterization

The main aim of this work was to synthesize the novel thiazole hydrazones and explore their biological potency. Herein, we prepared a novel thiazole hydrazones **5(a-h)** except **5e** [42, 43], by a simple two-step reaction. The

synthetic route is shown in Scheme 1, and the physical data summarized in Table 1 were obtained using various analytical techniques. The compounds' efficacy towards cytotoxicity and anti-inflammatory activity were determined.

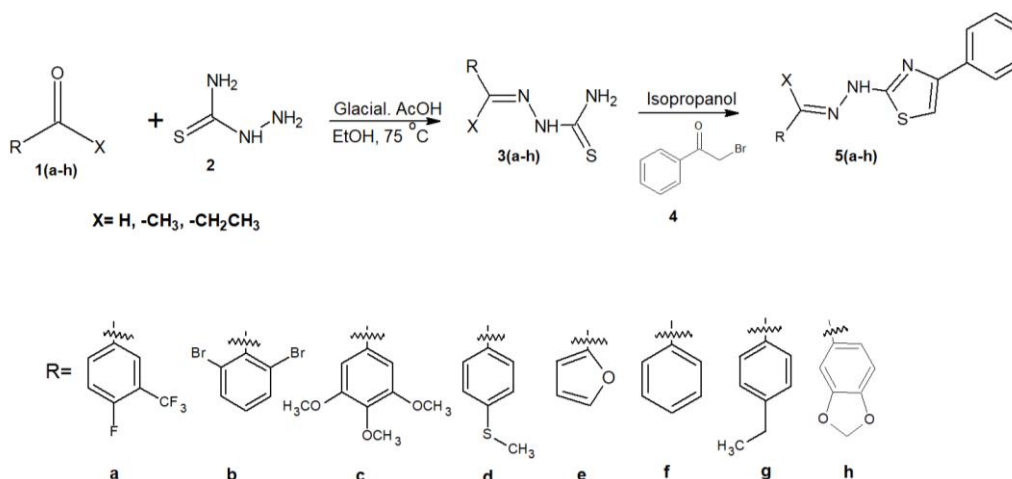
In the IR spectrum of compound **5a**, the signal at 3066 cm^{-1} was observed due to the presence of -NH functionality, the Ar-CH stretching occurs at 2939 cm^{-1} , the -C=N of hydrazone and thiazole resonated respectively at 1529 cm^{-1} and 1484 cm^{-1} , the peak at 1278 cm^{-1} is related to C-F stretching, and the C-S group resonated at 709 cm^{-1} .

In the ^1H NMR spectra of conjugate **5a**, the -NH proton resonated at δ 12.40 ppm as a broad singlet, the aromatic proton of -CH=N= functionality appeared at δ 8.01 ppm as a singlet, the signal at δ 7.36 ppm is related to the proton of thiazole ring and the aromatic protons were observed in the region 7.29–8.06 ppm as a multiplet. In the proton decoupled ^{13}C NMR spectra, the thiazole ring carbon resonated at δ 168.01 ppm, the aromatic carbons resonated in the region 117–160 ppm, and the azomethine carbon resonated at δ 105 ppm.

The mass spectra of compound **5a** confirmed the formation of the product by demonstrating a M^+ signal at m/z 365.8, which corresponds to a calculated molecular weight of the compound. The IR, ^1H NMR, ^{13}C NMR and mass spectra of all the synthesized thiazole derivatives **5(a-h)** are shown in the supplementary material (Figure S1–Figure S32).

3.2. Solvatochromic UV-Vis absorption

Figure 1 and Figure 2 show the UV-Vis absorption spectra of the synthesized conjugates, and Table 2 lists the specific spectral data. The maximum absorption of these compounds was found in the range of 326–366 nm in the UV-visible spectra. The π - π^* transition of electrons in aromatic rings present in all derivatives may account for this absorption [44]. On conjugation with aromatic rings, there is an abundance of electrons, resulting in a bathochromic shift. The compounds **5a** and **5d** exhibited bathochromic shift, as compared to the other synthesized compounds, and the compounds **5f** and **5g** showed a blue shift related to the other synthesized conjugates.



Scheme 1 Synthesis of thiazole hydrazone conjugates **5(a-h)**.

Table 1 Analytical data of the synthesized thiazole derivatives **5(a-h)**.

Compound	Structure	Molecular formula	Molecular weight	Yield (%)	m.p. (°C)
5a		C ₁₇ H ₁₁ F ₄ N ₃ S	365.3479	88	187–189
5b		C ₁₆ H ₁₁ Br ₂ N ₃ S	437.1516	90	192–193
5c		C ₁₇ H ₁₃ N ₃ OS	307.3692	86	171–173
5d		C ₁₇ H ₁₅ N ₃ S ₂	325.4511	92	189–191
5e		C ₁₅ H ₁₃ N ₃ OS	283.3482	89	135–136
5f		C ₁₈ H ₁₇ N ₃ S	307.4126	91	159–160
5g		C ₁₉ H ₁₉ N ₃ S	321.4392	88	201–203
5h		C ₁₈ H ₁₅ N ₃ O ₂ S	337.3956	92	123–124

The values of λ_{\max} for the synthesized thiazole compounds vary depending on the nature of the solvents and change with changing solvent polarity; among the ten solvents, the largest λ_{\max} was observed for any given compound in DMF and DMSO solvents with high polarity. This demonstrates that synthesized compounds are exhibiting solvatochromic behavior, which is attributed to the interaction of the solvent and lone pair electrons of azo dyes.

3.3. Computational studies

The optimized structures of the synthesized thiazole-conjugates are shown in the supplementary material (Figure S33–Figure S40). Figure 3 and Figure 4 display the energy

gap and electronic distribution of HOMO-LUMO of the synthesized thiazole hydrazones **5(a-h)**. As can be seen from the figures, compound **5a** has less energy gap, viz., 3.512 eV; soft molecule and the compound **5g** was found to have a large energy gap, viz., 4.38 eV. With the help of the energy of frontier molecular orbitals, some of the quantum chemical parameters were calculated using the following equations, and the values are listed in Table 3.

$$\text{Electronegativity } (\chi) = -1/2(E_{\text{LUMO}} + E_{\text{HOMO}}).$$

$$\text{Chemical potential } (\mu) = -\chi = 1/2(E_{\text{LUMO}} + E_{\text{HOMO}}).$$

$$\text{Global hardness } (\eta) = 1/2(E_{\text{LUMO}} - E_{\text{HOMO}}).$$

$$\text{Global softness } (S) = 1/2\eta.$$

$$\text{Electrophilicity index } (\omega) = \mu^2/2\eta.$$

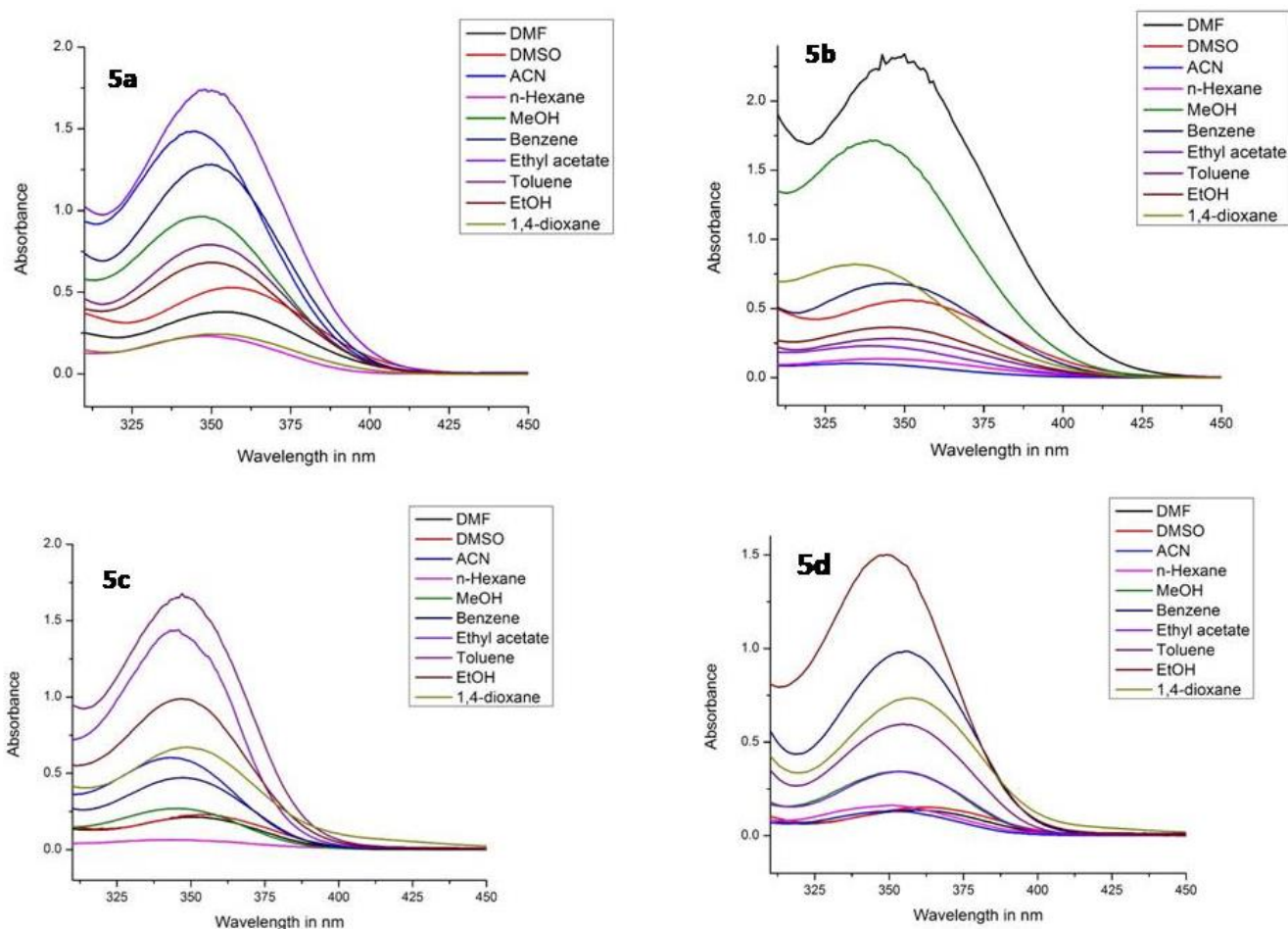


Figure 1 Solvatochromic absorption spectra of compounds 5(a-d).

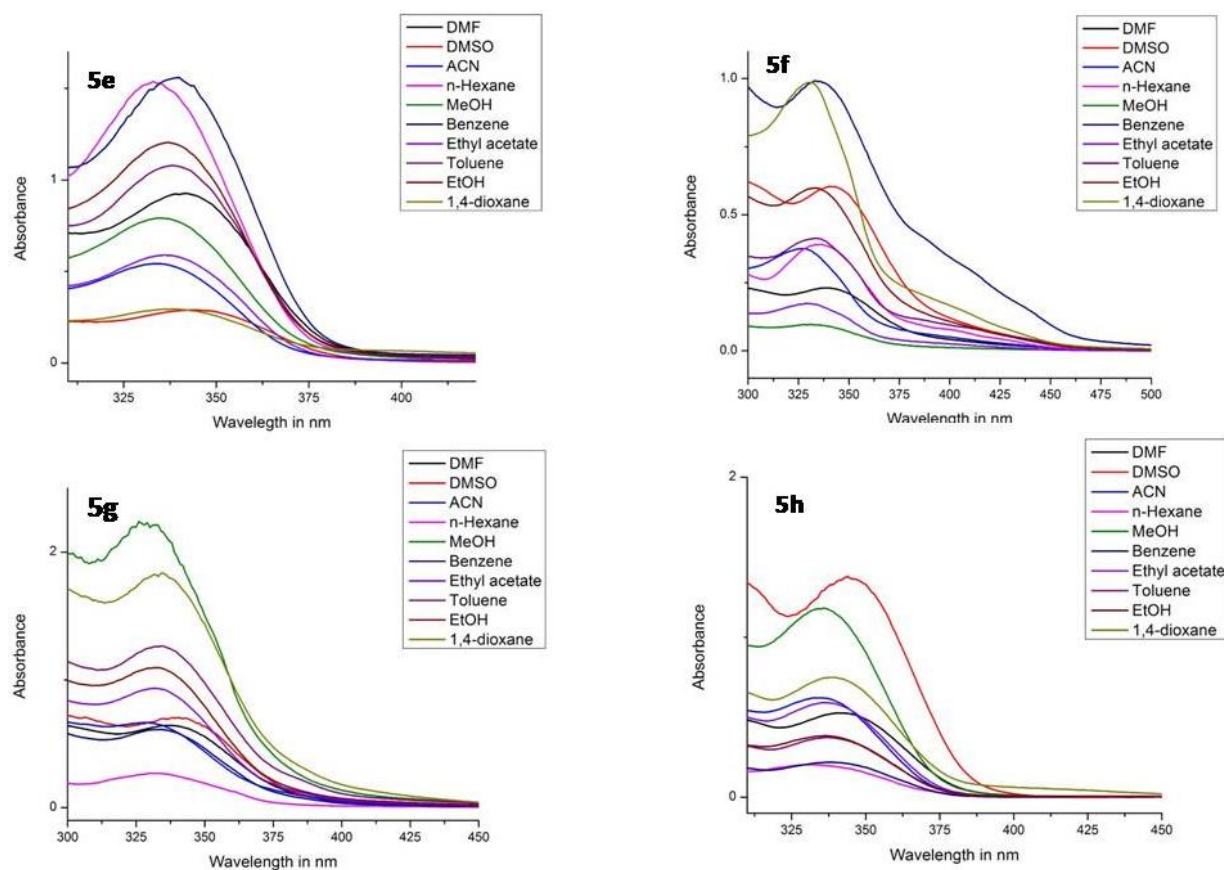


Figure 2 Solvatochromic absorption spectra of compounds 5(e-h).

Table 2 UV-Visible data of the synthesized compounds **5(a-h)**.

Compounds	λ_{\max} , nm									
	DMF	DMSO	ACN	n-Hexane	MeOH	Benzene	Ethyl acetate	Toluene	EtOH	1,4-dioxane
5a	353.63	355.29	342.83	348.63	346.42	349.75	348.09	348.92	349.18	353.63
5b	349.75	352.51	346.97	347.25	338.96	346.13	342.00	345.59	346.42	336.17
5c	350.59	356.96	343.92	343.09	346.97	347.25	344.75	346.42	346.97	348.92
5d	358.34	366.38	353.08	350.84	351.67	355.84	355.29	354.46	349.18	357.22
5e	341.23	346.90	334.49	332.75	336.00	339.70	337.31	338.19	337.31	339.04
5f	338.58	341.37	326.31	336.97	335.42	334.23	330.66	334.23	331.85	331.07
5g	338.71	340.50	330.41	333.08	328.35	334.29	331.88	334.56	330.72	334.29
5h	345.04	344.47	334.76	330.08	335.05	338.96	337.29	337.00	337.55	338.67

Compounds	Log ϵ									
	DMF	DMSO	ACN	n-Hexane	MeOH	Benzene	Ethyl acetate	Toluene	EtOH	1,4-dioxane
5a	3.58	3.72	4.17	3.36	3.98	4.10	4.24	3.89	3.85	3.39
5b	4.36	3.74	2.93	3.15	4.23	3.83	3.36	3.45	3.57	3.91
5c	3.32	3.36	3.77	2.80	3.43	3.67	4.15	4.22	3.99	3.83
5d	3.14	3.18	3.11	3.20	3.53	3.97	3.53	3.77	4.17	3.86
5e	3.96	3.46	3.73	4.18	3.89	4.19	3.77	4.03	4.07	3.47
5f	3.36	3.78	3.57	3.58	2.97	3.99	3.24	3.62	3.77	3.99
5g	3.81	3.84	3.82	3.41	4.34	3.78	3.97	4.10	4.03	4.26
5h	3.72	4.13	3.79	3.30	4.07	3.35	3.77	3.57	3.58	3.87

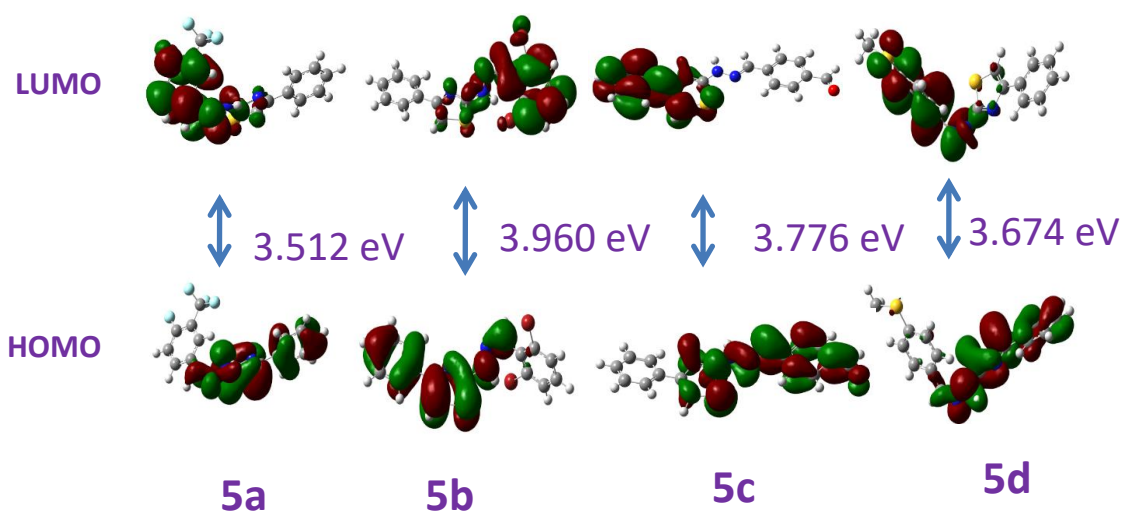
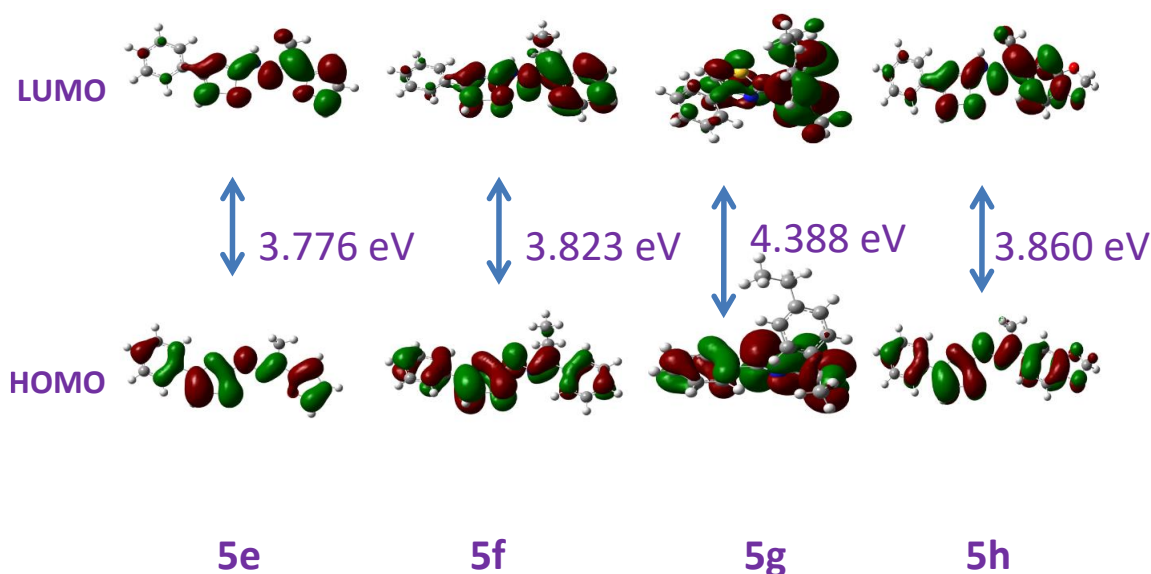
**Figure 3** Calculated FMO orbitals plot of the synthesized compounds **5(a-d)**.**Figure 4** Calculated FMO orbitals plot of the synthesized compounds **5(e-h)**.

Table 3 Quantum chemical parameters calculated for synthesized compounds **5(a-h)**.

Parameters	5a	5b	5c	5d	5e	5f	5g	5h
E_{HOMO} (eV)	-5.918	-5.680	-5.839	-5.623	-5.418	-5.517	-5.552	-5.429
E_{LUMO} (eV)	-2.406	-1.720	-2.063	-1.984	-1.642	-1.693	-1.163	-1.568
Energy gap (Δ) (eV)	3.512	3.960	3.776	3.674	3.776	3.823	4.388	3.860
Ionization energy (I) (eV)	5.918	5.680	5.839	5.623	5.418	5.517	5.552	5.429
Electron affinity (A) (eV)	2.406	1.720	2.063	1.984	1.642	1.693	1.163	1.568
Electronegativity (χ) (eV)	4.162	3.70	3.951	3.803	3.530	2.758	3.357	3.498
Chemical potential (μ) (eV)	-4.162	-3.70	-3.951	-3.803	-3.530	-2.758	-3.357	-3.498
Global hardness (η) (eV)	1.756	1.98	1.888	1.819	1.888	1.065	2.194	1.930
Global softness (S) (eV^{-1})	0.284	0.252	0.264	0.274	0.264	0.469	0.227	0.259
Electrophilicity index (ω) (eV)	4.932	3.457	4.134	3.974	3.30	3.571	2.567	3.169

Molecular electrostatic potential map (MEP) helps to predict the charge distribution in the molecule. In the MEP, the electrophilic nature of the molecule is represented by the positive regions (blue), and the nucleophilic nature of the molecule is represented by the negative regions (red). The MEP map was displayed in Figure 5, which reveals that the blue region was found at $-\text{NH}$ of the hydrazone in the synthesized compounds **5(a-h)**, and the red region was observed in compounds **5(c-f)**.

3.4. Biological activity

3.4.1. Antimicrobial activity

The inhibition efficacy of the synthesized compounds **5(a-h)** towards both gram-positive and gram-negative bacterial strains was determined by the disc diffusion method using DMSO, even though DMSO is toxic to antimicrobial strains, but to a lesser extent [44], and the results were appended in Table 4. The compounds **5c**, **5d**, and **5g** showed excellent activity compared to *Escherichia coli*, *Pseudomonas aeruginosa*, *Staphylococcus aureus*, and *Bacillus Subtilis* compared to streptomycin, and the remaining compounds showed moderate to good activity.

The antifungal activities of the titled compounds **5(a-h)** towards fungal strains such as *Aspergillus flavus*, *Candida albicans* and *Aspergillus terreus* are shown in Table 4. From the results, it was found that compounds **5a** and **5c** display a good activity against *Aspergillus flavus* and *Candida albicans*. Furthermore, the remaining derivatives also show significant activity.

3.4.2. Cytotoxic activity

All the synthesized thiazole derivatives were screened for their cytotoxic activity against MCF-7 and HePG2 cell lines. The IC_{50} values for cytotoxic activity of the synthesized compounds are listed in Table 5, and the % cell viability against the treated compounds is shown in Figure 6 and Figure 7. Compounds **5c** and **5f** inhibited MCF-7 cell lines to a good extent with IC_{50} values 58.13 $\mu\text{g}/\text{mL}$ and 60.88 $\mu\text{g}/\text{mL}$, respectively; compounds **5h** and **5d** displayed excellent activity against HePG2 cells with IC_{50} values 55.8 $\mu\text{g}/\text{mL}$ and 57.47 $\mu\text{g}/\text{mL}$, respectively, and the remaining compounds exhibited moderate activity against both

MCF-7 and HePG2 cells with the IC_{50} values ranging from 61.80 to 70.08 $\mu\text{g}/\text{mL}$.

3.4.3. Anti-inflammatory activity

The anti-inflammatory efficacy of the synthesized derivatives **5(a-h)** was determined against MMP-2 and MMP-9, and results were interpreted in terms of % inhibition. The % inhibition of the synthesized compounds is shown in Table 6. Gelatin Zymography image is shown in Figure 8. From Table 6, it can be noticed that compound **5c** indicates very good efficacy, viz., inhibited MMP-2 and MMP-9 to 70% and 55% respectively. Compound **5f** exhibits lower activity against both MMP-2 and MMP-9 compared to the other compounds. The remaining compounds exhibit moderate activity.

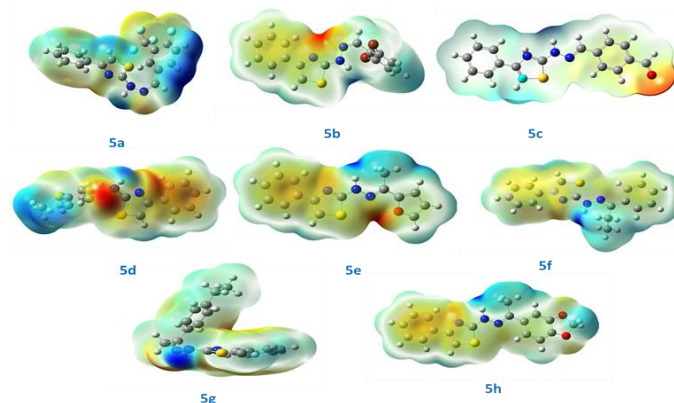
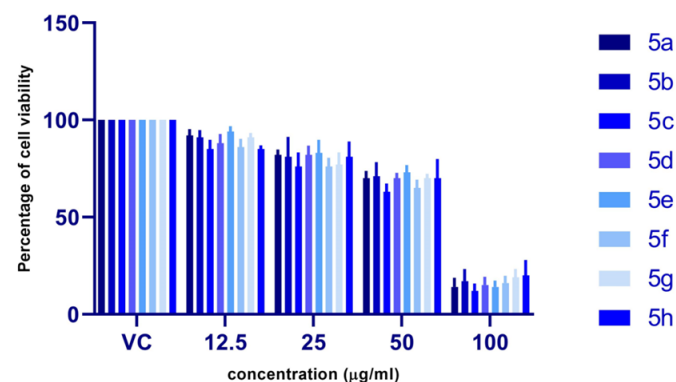
**Figure 5** MEP map of the synthesized compounds **5(a-h)**.**Figure 6** MCF-7 Cell viability % against the synthesized thiazole conjugates **5(a-h)**.

Table 4 Antimicrobial activity results of synthesized compounds **5(a-h)**.

Compounds	Concentration, mg/mL	Zone of inhibition in mm (mean \pm S.D.)							
		Bacterial strains				Fungal strains			
		<i>P. a.</i>	<i>B. s.</i>	<i>S. t.</i>	<i>E. c.</i>	<i>A. f.</i>	<i>C. a.</i>	<i>M. g.</i>	<i>A. t.</i>
5a	1	18 \pm 0.4	19 \pm 0.3	15 \pm 0.2	17 \pm 0.4	20 \pm 0.45	16 \pm 0.7	19 \pm 0.2	21 \pm 0.53
	0.5	12 \pm 0.2	11 \pm 0.4	16 \pm 0.5	14 \pm 0.6	15 \pm 0.2	15 \pm 0.9	16 \pm 0.2	17 \pm 0.3
5b	1	16 \pm 0.36	17 \pm 0.25	20 \pm 0.4	19 \pm 0.2	19 \pm 0.43	20 \pm 0.4	21 \pm 0.4	18 \pm 0.5
	0.5	14 \pm 0.23	13 \pm 0.5	17 \pm 0.34	16 \pm 0.24	15 \pm 0.32	14 \pm 0.5	16 \pm 0.3	13 \pm 0.53
5c	1	23 \pm 0.4	21 \pm 0.3	19 \pm 0.6	20 \pm 0.5	21 \pm 0.3	17 \pm 0.4	19 \pm 0.6	18 \pm 0.4
	0.5	14 \pm 0.52	13 \pm 0.3	11 \pm 0.5	12 \pm 0.6	11 \pm 0.32	13 \pm 0.4	11 \pm 0.6	12 \pm 0.6
5d	1	20 \pm 0.4	19 \pm 0.6	17 \pm 0.4	18 \pm 0.4	19 \pm 0.25	18 \pm 0.36	17 \pm 0.4	18 \pm 0.6
	0.5	13 \pm 0.1	16 \pm 0.54	14 \pm 0.24	15 \pm 0.45	12 \pm 0.5	11 \pm 0.23	15 \pm 0.4	14 \pm 0.3
5e	1	17 \pm 0.5	15 \pm 0.4	14 \pm 0.4	19 \pm 0.7	18 \pm 0.5	15 \pm 0.23	19 \pm 0.6	18 \pm 0.4
	0.5	12 \pm 0.3	13 \pm 0.1	12 \pm 0.4	11 \pm 0.7	14 \pm 0.35	11 \pm 0.5	13 \pm 0.1	12 \pm 0.5
5f	1	12 \pm 0.4	11 \pm 0.31	13 \pm 0.5	11 \pm 0.6	13 \pm 0.32	10 \pm 0.3	15 \pm 0.6	14 \pm 0.4
	0.5	09 \pm 0.6	10 \pm 0.3	12 \pm 0.4	10 \pm 0.4	10 \pm 0.5	12 \pm 0.3	08 \pm 0.25	12 \pm 0.6
5g	1	20 \pm 0.25	21 \pm 0.16	19 \pm 0.44	20 \pm 0.6	17 \pm 0.5	20 \pm 0.1	19 \pm 0.25	20 \pm 0.26
	0.5	14 \pm 0.36	17 \pm 0.3	11 \pm 0.5	23 \pm 0.4	12 \pm 0.4	20 \pm 0.2	15 \pm 0.4	16 \pm 0.22
5h	1	16 \pm 0.4	17 \pm 0.5	19 \pm 0.4	15 \pm 0.41	16 \pm 0.4	21 \pm 0.46	19 \pm 0.51	17 \pm 0.3
	0.5	10 \pm 0.1	15 \pm 0.21	13 \pm 0.5	10 \pm 0.24	12 \pm 0.4	15 \pm 0.4	12 \pm 0.6	13 \pm 0.5
Standard^a		23 \pm 0.6	22 \pm 0.3	21 \pm 0.4	20 \pm 0.3	-	-	-	-
Standard^b		-	-	-	-	22 \pm 0.3	21 \pm 0.5	20 \pm 0.4	22 \pm 0.2

P. a - *Pseudomonas aeruginosa*, *B. s* - *Bacillus Subtilis*, *E. s* - *Escherichia coli*, *S. a* - *Staphylococcus aureus*, *A. f* - *Aspergillus flavus*, *C. a* - *Candida albicans*, *A. s* - *Aspergillus terreus*, *A. t* - *Aspergillus terreus*.

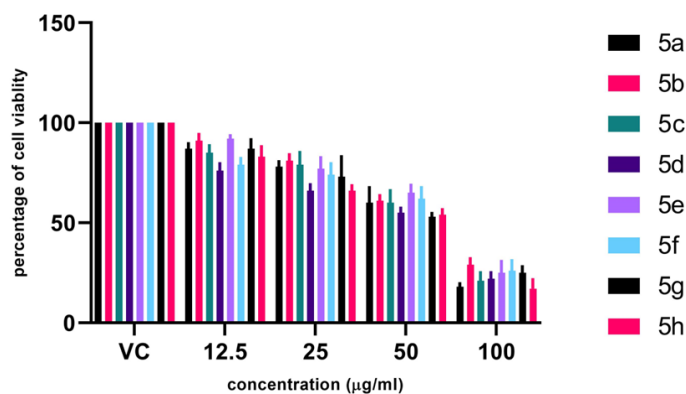
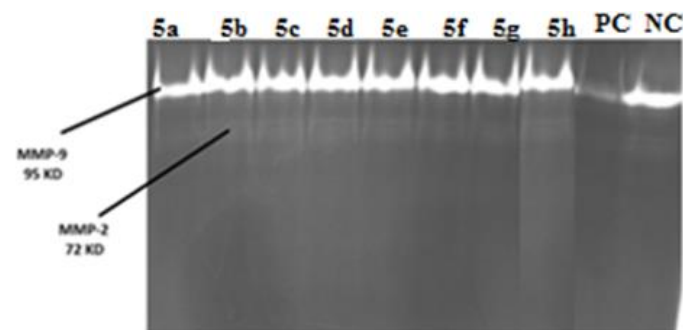
Standard^a - Streptomycin, Standard^b - Fluconazole.

Table 5 IC₅₀ values of the synthesized compounds against MCF-7 and HePG2 cell lines.

Compounds	IC ₅₀ in μ g/mL against MCF-7 cells	IC ₅₀ in μ g/mL against HePG2 cells
5a	62.35	61.02
5b	65.43	70.02
5c	58.13	62.6
5d	63.36	57.47
5e	64.48	67.31
5f	60.88	64.57
5g	64.54	61.8
5h	63.03	55.8

Table 6 Anti-inflammatory activity of the synthesized compounds **5(a-h)**.

S.NO.	Name of the compound	MMP-2 (% Inhibition)	MMP-9 (% Inhibition)
1	5a	55	15
2	5b	50	30
3	5c	70	55
4	5d	60	20
5	5e	65	15
6	5f	20	15
7	5g	70	30
8	5h	30	10
9	PC (positive control)	100	95
10	NC (negative control)	o(NIL)	o(NIL)

**Figure 7** HePG2 Cell viability % against the synthesized thiazole conjugates **5(a-h)**.**Figure 8** Gelatin Zymography showing MMP-2 and MMP-9 treated with synthesized derivatives **5(a-h)**.

3.4.4. *In silico* Molecular docking study

To support the *in vitro* biological activity of the synthesized thiazole-hydrazone conjugates, *in silico* molecular docking study was carried out with COX-2 receptor (PDB:1PXX). The binding energy, number of hydrogen bonds and the hydrophobic interaction of the compounds with receptors are tabulated in Table 7. The 2D and 3D view of the interaction of synthesized compounds with COX-2 is given in Figure 9. From the *in silico* study results, it was found that all the compounds showed excellent binding affinity in the range of -6.9 to -8.4 kcal/mol compared to standard drug diclofenac (-8.4 kcal/mol). Compounds **5d**, **5f**, and **5g** exhibited hydrogen bonds, but the remaining compounds did not show hydrogen bond. All compounds displayed hydrophobic interactions with the COX-2 receptor.

4. Limitations

The authors did not find any difficulties and limitations during this research work.

5. Conclusions

Herein we reported the synthesis of thiazole-hydrazone conjugates **5(a-h)**, and their structure was identified with the help of analytical techniques such as UV, IR NMR and mass spectrometry. In addition, global and reactive parameters were calculated via the computational study. All the synthesized compounds exhibit positive solvatochromic behaviour, significant potency towards antibacterial activity, excellent efficacy toward cytotoxins and anti-inflammatory activity. Furthermore, the synthesized compounds showed a good docking score with the COX-2 receptor.

• Supplementary materials

This manuscript contains supplementary materials, which are available on the corresponding online page.

• Funding

This research had no external funding.

Table 7 Molecular docking results of synthesized thiazole-conjugates **5(a-h)** and diclofenac with COX-2 receptor.

Ligand	Hydrogen bonds	Bond length (Å)	H-Bond With	Hydrophobic interactions	Binding energy (kcal/mol)
5a	0			Met 113, Arg 120, Ile 345, Leu 531, Phe 518, Val 349, Met 522, Leu 352, Val 523, Gly 526, Tyr 385, Phe 381, Leu 384, Trp 387, Tyr 355, Ser 353, Leu 359, Val 116, Met 113	-8.4
5b	0			Leu 359, Val 116, Met 113, Val 349, Ser 353, Val 523, Phe 381, Gly 526, Tyr 385, Met 522, Leu 384, Trp 387, Ala 527, Leu 531, Ile 345	-8.0
5c	0			Phe 518, Val 253, Gln 192, Ala 516, Ala 527, Ser 253, His 90, Val 116, Val 349, Arg 120, Leu 531, Ser 530, Leu 352	-6.9
5d	1	3.1	Drg:N2:Tyr 355OB	Ala 516, Ser 353, His 90, Arg 513, Leu 352, Val 523, Phe 518, Ser 530, Tyr 385, Tyr 348, Gly 526, Ala 527, Val 349, Leu 531	-7.5
5e	0			Tyr 385, Leu 384, Trp 387, Gly 526, Val 523, Ala 527, Leu 531, Met 113, Leu 359, Tyr 385, Val 349, Tyr 355, Val 116, Ser 353, Phe 518, Leu 352, Trp 387, Met 522	-7.9
5f	2	3.12 2.91	Drg:E:Tyr 355OB Drg:E:Arg 120 NB1	Phe 518, Leu 352, Trp 387, Gly 526, Val 523, Ala 527, Phe 381, Leu 384, Tyr 385, Met 522, Ile 345, Met 113, Val 349, Leu 531, Leu 359, Ser 353	-7.6
5g	1	2.88	Drg:N1:Tyr 385 OH	Val 349, Leu 352, Tyr 348, Ser 530, Leu 534, Phe 205, Ile 377, Val 228, Phe 381, Phe 381, Phe 209, Gly 533, Val 344, Ala 527, Leu 531	-6.9
5h	0			Phe 369, Trp 194, Leu 209, Tyr 489	-7.9
Diclofenac	2	2.87 2.82	Drg:N1:Tyr 385 OH Drg:N1:Tyr 385 OH	Leu 384, Gly 526, Phe 518, Trp 387, Ser 353, Val 523, Met 522, Tyr 355, Ala 527, Leu 352, Val 349, Tyr 348,	-8.4

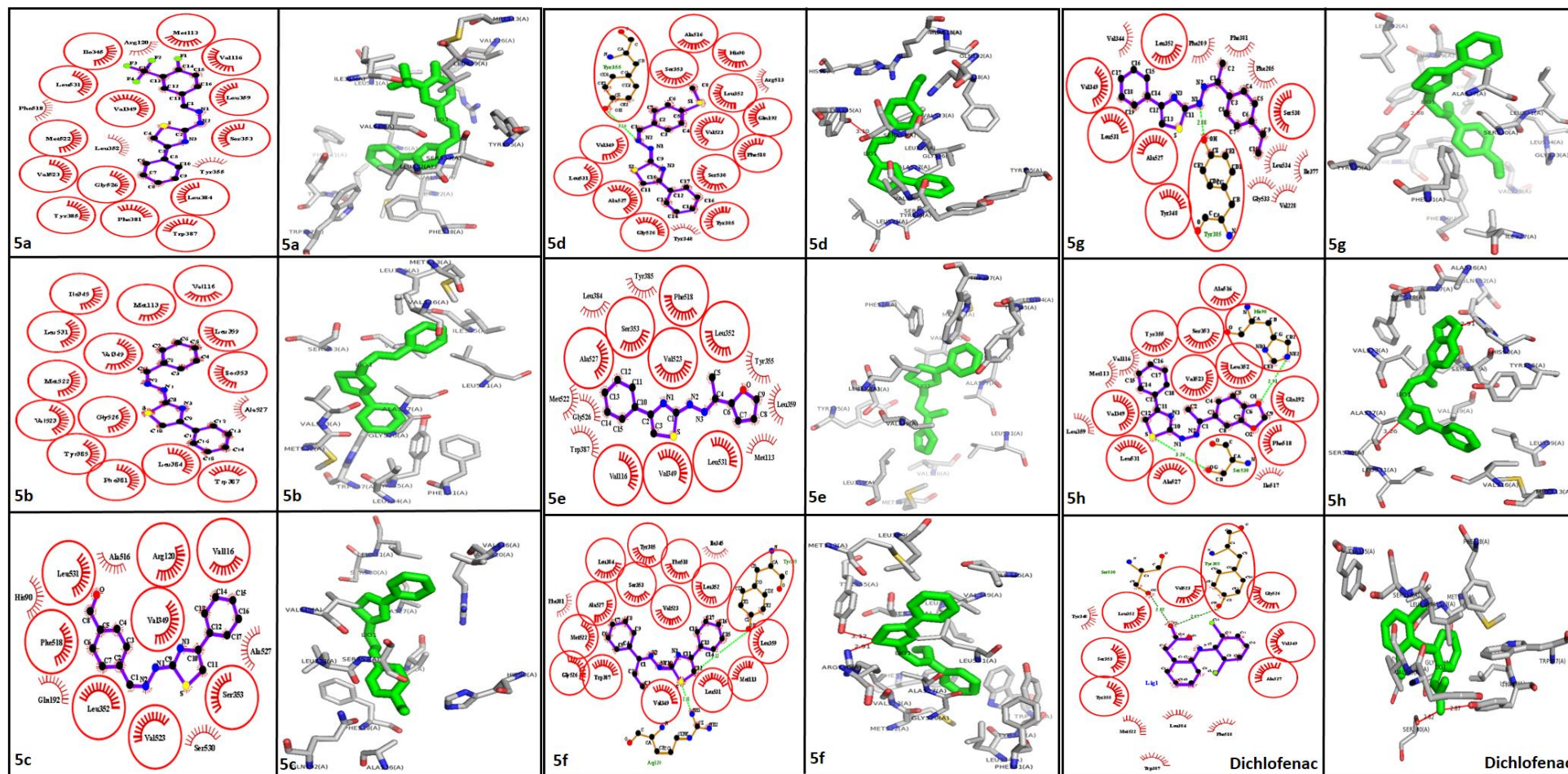


Figure 9 2D and 3D docked view of compounds 5(a-h) and diclofenac with COX-2 receptor.

● Author contributions

Conceptualization: N.B.P.

Data curation: K.Y.C.

Formal Analysis: K.Y.C., N.B.P., M.P.K.

Funding acquisition: N.B.P., M.P.K.

Investigation: K.Y.C., M.P.K.

Methodology: K.Y.C., N.B.P., M.P.K.

Project administration: M.P.K.

Resources: K. K.Y.C., Y.C., N.B.P.

Software: K.Y.C., M.P.K.

Supervision: M.P.K.

Validation: K.Y.C., M.P.K.

Visualization: M.P.K.

Writing – original draft: K.Y.C., N.B.P.

Writing – review & editing: M.P.K.

● Conflict of interest

The authors declare no conflict of interest.

● Additional information

Author IDs:

BP Nandeshwarappa, Scopus ID [11839628200](https://orcid.org/11839628200);

KM Mussuvir Pasha, Scopus ID [57416747400](https://orcid.org/57416747400).

Websites:

Davangere University, <https://vskub.ac.in>;

Vijayanagara Sri Krishnadevaraya University, <https://davangereuniversity.ac.in>.

References

- Mallikarjuna SM, Padmashali MSMB, Chandrashekarappa S, Sandeep C. Synthesis, anticancer and antituberculosis studies for [1-(4-chlorophenyl) Cyclopropyl](Piperazine-yl) Methanone derivatives. *Int J Pharm Sci Res.* 2014;6(7):423–427.
- Nagesh HK, Padmashali B, Sandeep C, Musturappa TE, Lokesh M. Synthesis and characterization of novel benzothio-phenone substituted oxadiazole derivatives and their antimicrobial activity. *Pharma Chem.* 2015;7:129–136.
- Pattanashetty SH, Hosamani, KM, Barretto DA. Microwave assisted synthesis, computational study and biological evaluation of novel quinolin-2 (1H)-one based pyrazoline hybrids. *Chem Data Coll.* 2018;15:184–196. doi:[10.1016/j.cdc.2018.06.003](https://doi.org/10.1016/j.cdc.2018.06.003)
- Pattanashetty SH, Hosamani KM, Shettar AK, Mohammed Shafeeulla R. Design, synthesis and computational studies of novel carbazole n-phenylacetamide hybrids as potent antibacterial, anti-inflammatory, and antioxidant agents. *Synth Commun.* 2018;55:1765–1774. doi:[10.1080/00397911.2019.1620281](https://doi.org/10.1080/00397911.2019.1620281)
- Nandeshwarappa BP, Chandrashekarappa S, Ningegowda R, Selenium-containing heterocycles: Synthetic investigation of some new series 3-(5-mercapto-1, 3, 4-oxadiazol-2-yl)-2H-selenopyrano [2, 3-b] quinolin-2-ones. *Chem Data Collec.* 2020;29:100510. doi:[10.1016/j.cdc.2020.100510](https://doi.org/10.1016/j.cdc.2020.100510)
- Chen L, Liu XY, Zou YX. Recent advances in the construction of phosphorus-substituted heterocycles. *Adv Synth Catal.* 2020;362:1724–1818. doi:[10.1002/adsc.201901540](https://doi.org/10.1002/adsc.201901540)
- Khatoon H, Abdulmalek E. A focused review of synthetic applications of lawesson's reagent in organic synthesis. *Mol.* 2021;26:6937. doi:[10.3390/molecules26226937](https://doi.org/10.3390/molecules26226937)
- Sharma PC, Bansal KK, Sharma A, Sharma D, Deep A. Thiazole-containing compounds as therapeutic targets for cancer therapy. *Eur J Med Chem.* 2020;188:112016. doi:[10.1016/j.ejmech.2019.112016](https://doi.org/10.1016/j.ejmech.2019.112016)
- Ashwani Kumar, Anup Pandith, Hong-Seok Kim, Pyrene-appended imidazolium probe for 2,4,6-trinitrophenol in water. *Sensors Actuators B Chem.* 2016;231:293–301. doi:[10.1016/j.snb.2016.03.033](https://doi.org/10.1016/j.snb.2016.03.033)
- Prakashiah BG, Vinaya Kumara D, Anup Pandith A, Nityananda Shetty A, Amitha Rani BE. Corrosion inhibition of 2024-T3 aluminum alloy in 3.5% NaCl by thiosemicarbazone derivatives. *Corros Sci.* 2018;136:326–338. doi:[10.1016/j.corsci.2018.03.021](https://doi.org/10.1016/j.corsci.2018.03.021)
- Pathania S, Narang RK, Rawal RK. Role of sulphur-heterocycles in medicinal chemistry: An update. *Eur J Med Chem.* 2019;180:486–508. doi:[10.1016/j.ejmech.2019.07.043](https://doi.org/10.1016/j.ejmech.2019.07.043)
- Matiadis D, Sagnou M. Pyrazoline hybrids as promising anti-cancer agents: An up-to-date overview. *Int J Mol Sci.* 2020;21:5507. doi:[10.3390/ijms21155507](https://doi.org/10.3390/ijms21155507)
- Pereira PS, de Lima MDCA, Neto PPM, de Moraes Oliveira-Tintino CD, Tintino SR, de Alencar Menezes IR, Silva TG. Thiazolidinedione and thiazole derivatives potentiate norfloxacin activity against NorA efflux pump over expression in *Staphylococcus aureus* 1199B strains. *Bioorg Med Chem.* 2019;27:3797–3804. doi:[10.1016/j.bmc.2019.07.006](https://doi.org/10.1016/j.bmc.2019.07.006)
- Ankali KN, Rangaswamy J, Shalavadi M, Naik N, Naik Krishnamurthy G. Synthesis and molecular docking of novel 1, 3-thiazole derived 1, 2, 3-triazoles and in vivo biological evaluation for their anti anxiety and anti inflammatory activity. *J Mol Struct.* 2021;123:130357. doi:[10.1016/j.molstruc.2021.130357](https://doi.org/10.1016/j.molstruc.2021.130357)
- Gürsoy E, Dincel ED, Naesens L, Güzeldemirci NU. Design and synthesis of novel imidazo [2, 1-b] thiazole derivatives as potent antiviral and antimycobacterial agents. *Bioorg Chem.* 2020;95:103496. doi:[10.1016/j.bioorg.2019.103496](https://doi.org/10.1016/j.bioorg.2019.103496)
- Eissa SI, Farrag AM, Abbas SY, El Shehry MF, Ragab A, Fayed EA, Ammar YA. Novel structural hybrids of quinoline and thiazole moieties: Synthesis and evaluation of antibacterial and antifungal activities with molecular modeling studies. *Bioorg Chem.* 2021;110:104803. doi:[10.1016/j.bioorg.2021.104803](https://doi.org/10.1016/j.bioorg.2021.104803)
- De Santana TI, de Oliveira Barbosa M, de Moraes Gomes PAT, da Cruz ACN, da Silva TG, Leite ACL. Synthesis, anticancer activity and mechanism of action of new thiazole derivatives. *Eur J Med Chem.* 2018;144:874–886. doi:[10.1016/j.ejmech.2017.12.040](https://doi.org/10.1016/j.ejmech.2017.12.040)
- Kumar G, Singh NP. Synthesis, anti-inflammatory and analgesic evaluation of thiazole/oxazole substituted benzothiazole derivatives. *Bioorg Chem.* 2021;107:104608. doi:[10.1016/j.bioorg.2020.104608](https://doi.org/10.1016/j.bioorg.2020.104608)
- Eryılmaz S, Çelikoğlu ET, İdil Ö, İnkaya E, Kozak Z, Mısırlı E, Gül M. Derivatives of pyridine and thiazole hybrid: Synthesis, DFT, biological evaluation via antimicrobial and DNA cleavage activity. *Bioorg Chem.* 2020;95:103476. doi:[10.1016/j.bioorg.2019.103476](https://doi.org/10.1016/j.bioorg.2019.103476)
- Cuevas JM, Seoane-Rivero R, Navarro R, Marcos-Fernández Á. Coumarins into polyurethanes for smart and functional materials. *Polym.* 2020;12:630. doi:[10.3390/polym12030630](https://doi.org/10.3390/polym12030630)
- Eltyshev AK, Dzhumaniyazov TH, Suntsova PO, Minin AS, Pozdina VA, Dehaen W, Belskaya NP. 3-Aryl-2-(thiazol-2-yl) acrylonitriles assembled with aryl/hetaryl rings: design of the optical properties and application prospects. *Dyes Pigment.* 2021;184:108836. doi:[10.1016/j.dyepig.2020.108836](https://doi.org/10.1016/j.dyepig.2020.108836)
- Godugu K, Shaik S, Pinjari MKM, Gundala TR, Subramanyam DVC, Loka SS, Nallagonda CGR. Solid state thiazole-based fluorophores: Promising materials for white organic light emitting devices. *Dyes Pigment.* 2021;187:109077. doi:[10.1016/j.dyepig.2020.109077](https://doi.org/10.1016/j.dyepig.2020.109077)
- Godugu K, Shaik S, Pinjari MKM, Gundala TR, Subramanyam DVC, Loka SS, Nallagonda CGR. Solid state thiazole-based

- fluorophores: promising materials for white organic light emitting devices. *Dyes Pigment.* 2021;187:109077. doi:[10.1016/j.dyepig.2020.109077](https://doi.org/10.1016/j.dyepig.2020.109077)
24. Nandeshwarappa BP, Chandrashekarappa S, Sadashiv SO. Synthesis and antibacterial evaluation of 3-acetyl-2H-selenopyrano [2, 3-b] quinolin-2-ones. *Chem Data Collect.* 2020;28:100484-100495. doi:[10.1016/j.cdc.2020.100484](https://doi.org/10.1016/j.cdc.2020.100484)
25. Fazil S, Smitha M, Mary YS, Mary YS, Chandramohan V, Kumar N, Van Alsenoy C. Structural (SC-XRD), spectroscopic, DFT, MD investigations and molecular docking studies of a hydrazone derivative. *Chem Data Collect.* 2020;30:100588. doi:[10.1016/j.cdc.2020.100588](https://doi.org/10.1016/j.cdc.2020.100588)
26. Praveen Kumara CH, Katagi Manjunatha S, Nandeshwarappa BP. Synthesis of novel pyrazolic analogues of chalcones as potential antibacterial and antifungal agents. *Curr Chem Lett.* 2023;12:1. doi:[10.5267/j.ccl.2023.2.001](https://doi.org/10.5267/j.ccl.2023.2.001)
27. Tripathi RK, Ayyannan SR. Evaluation of 2-amino-6-nitrobenzothiazole derived hydrazones as acetylcholinesterase inhibitors: in vitro assays, molecular docking and theoretical ADMET prediction. *Med Chem Res.* 2018;27:709-725. doi:[10.1007/s00044-017-2095-3](https://doi.org/10.1007/s00044-017-2095-3)
28. Abu-Dief AM, El-khatib RM, El Sayed SM, Alzahrani S, Alkhatib F, El-Sarrag G, Ismael M. Tailoring structural elucidation, DFT calculation, DNA interaction and pharmaceutical applications of some aryl hydrazone Mn (II), Cu (II) and Fe (III) complexes. *J Mol Struct.* 2021;1244:131017. doi:[10.1016/j.molstruc.2021.131017](https://doi.org/10.1016/j.molstruc.2021.131017)
29. Gamov GA, Zavalishin MN, Petrova MV, Khokhlova AY, Gashnikova AV, Kiselev AN, Sharnin VA. Interaction of pyridoxal-derived hydrazones with anions and Co²⁺, Co³⁺, Ni²⁺, Zn²⁺ cations. *Phys Chem Liquid.* 2021;59:666-678. doi:[10.1080/00319104.2020.1774878](https://doi.org/10.1080/00319104.2020.1774878)
30. Frisch MJE, Trucks GW, Schlegel HB, Scuseria GE, Robb MA, Cheeseman CJR, Nakatsuji H. gaussian 09, Revision d. 01, Gaussian, Inc., Wallingford CT, 2009; 201 p.
31. Schlegel HB. Optimization of equilibrium geometries and transition structures. *J Comput Chem.* 1982;3:214-218. doi:[10.1002/jcc.540030212](https://doi.org/10.1002/jcc.540030212)
32. Ditchfield R, Miller DP, Pople JA. Self-consistent molecular orbital methods molecular orbital theory of NMR chemical shifts. *J Chem Phys.* 1971;54:4186-4193. doi:[10.1063/1.1674657](https://doi.org/10.1063/1.1674657)
33. Dennington R, Keith T, Millam J, GaussView, version 2009; 5.
34. Kumar CP, Katagi MS, Nandeshwarappa BP. Novel synthesis of quinoline chalcone derivatives-Design, synthesis, characterization and antimicrobial activity. *Chem Data Collect.* 2022;42:100955. doi:[10.1016/j.cdc.2022.100955](https://doi.org/10.1016/j.cdc.2022.100955)
35. Nandeshwarappa BP, Chandrashekarappa S, Prakash GK. Nitrogen and selenium containing heterocycles: Part-1: Synthesis of some new substituted 3-(5-(2-oxopropylthio)-1, 3, 4-oxadiazol-2-yl)-2H-selenopyrano [2, 3-b] quinolin-2-ones, *Chem Data Collect.* 2020;29:100534-100541. doi:[10.1016/j.cdc.2020.100534](https://doi.org/10.1016/j.cdc.2020.100534)
36. Kenchappa R, Bodke YD, Asha B, Telkar S, Sindhe MA. Synthesis, antimicrobial, and antioxidant activity of benzofuranbarbitone and benzofuranthiobarbitone derivatives. *Med Chem Res.* 2014;23:3065-3081. doi:[10.1007/s00044-013-0892-x](https://doi.org/10.1007/s00044-013-0892-x)
37. Mosmann T. Rapid colorimetric assay for cellular growth and survival: application to proliferation and cytotoxicity assays, *J I Meth.* 1983;65:55-63. doi:[10.1016/0022-1759\(83\)90303-4](https://doi.org/10.1016/0022-1759(83)90303-4)
38. Manjunatha B, Bodke YD, Jain R. Novel isoxazolone based azo dyes: synthesis, characterization, computational, solvatochromic UV-Vis absorption and biological studies. *J Mol Struct.* 2021;1244:130933. doi:[10.1016/j.molstruc.2021.130933](https://doi.org/10.1016/j.molstruc.2021.130933)
39. Schüttelkopf AW, Van Aalten DM. PRODRG: a tool for high-throughput crystallography of protein-ligand complexes. *Acta Crystallograph Sec D Biol Crystallograph.* 2004;60:1355-1363. doi:[10.1107/S0907444904011679](https://doi.org/10.1107/S0907444904011679)
40. Manjunatha B, Bodke YD, Kumaraswamy HM, Meghana P, Nagaraja O. Novel thioether linked 4-hydroxycoumarin derivatives: Synthesis, characterization, in vitro pharmacological investigation and molecular docking studies. *J Mol Struct.* 2022; 1249; 131642. doi:[10.1016/j.molstruc.2021.131642](https://doi.org/10.1016/j.molstruc.2021.131642)
41. Manjunatha B, Bodke YD, Nagaraja O, Nagaraju G, Sridhar MA. Coumarin-benzothiazole based azo dyes: synthesis, characterization, computational, photophysical and biological studies. *J Mol Struct.* 2021;1246:131170. doi:[10.1016/j.molstruc.2021.131170](https://doi.org/10.1016/j.molstruc.2021.131170)
42. Hassan AA, Ibrahim YR, El-Sheref EM, Abdel-Aziz M, Bräse S, & Nieger M. Synthesis and Antibacterial Activity of 4-Aryl-2-(1-substituted ethylidene) thiazoles. *Archiv der Pharmazie.* 2013;346:562-570. doi:[10.1002/ardp.201300099](https://doi.org/10.1002/ardp.201300099)
43. El-Naggar AM, El-Hashash MA, Elkadeeb EB. Eco-friendly sequential one-pot synthesis, molecular docking, and anti-cancer evaluation of arylidene-hydrazinyl-thiazole derivatives as CDK2 inhibitors. *Bioorg Chem.* 2015;108:104615. doi:[10.1016/j.bioorg.2020.104615](https://doi.org/10.1016/j.bioorg.2020.104615)
44. Kirkwood ZI, Millar BC, Downey DG, Moore JE. Antimicrobial effect of dimethyl sulfoxide and N, N-Dimethylformamide on Mycobacterium abscessus: implications for antimicrobial susceptibility testing. *Int J Mycobacteriol.* 2018;7:134. doi:[10.4103/ijmy.ijmy_35_18](https://doi.org/10.4103/ijmy.ijmy_35_18)
45. Dulian P, Nachit W, Jaglarz J, Zięba P, Kanak J, Żukowski W. Photocatalytic methylene blue degradation on multilayer transparent TiO₂ coatings. *Opt Mater (Amst).* 2019;90:264-272. doi:[10.1016/j.optmat.2019.02.041](https://doi.org/10.1016/j.optmat.2019.02.041)